Journal of Magnetic Resonance 206 (2010) 219–226

Contents lists available at ScienceDirect

Journal of Magnetic Resonance

journal homepage: www.elsevier.com/locate/jmr

PERFIDI filters to suppress and/or quantify relaxation time components in multi-component systems: An example for fat–water systems

V. Bortolotti [a], P. Fantazzini [b,*], M. Gombia [b], D. Greco [c], G. Rinaldin [b], S. Sykora [d]

[a] Department DICAM, University of Bologna, Viale Risorgimento 2, 40136 Bologna, Italy
[b] Department of Physics, University of Bologna, Viale Berti Pichat 6/2, 40127 Bologna, Italy
[c] ESAOTE S.p.A. Via A. Siffredi 58, 16153 Genova, Italy
[d] Extra Byte, Via Raffaello Sanzio 22/c, 20022 Castano Primo (MI), Italy

ARTICLE INFO

Article history:
Received 7 May 2010
Revised 8 July 2010
Available online 18 July 2010

Keywords:
NMR
MRI
PERFIDI
Relaxation filters
Inversion pulse
Spectroscopy
Imaging
Relaxometry
T_1
Inverse Laplace Transform
Fat suppression

ABSTRACT

Parametrically Enabled Relaxation FIlters with Double and multiple Inversion (PERFIDI) is an experimental NMR/MRI technique devised to analyze samples/voxels characterized by multi-exponential longitudinal relaxation. It is based on a linear combination of NMR sequences with suitable preambles composed of inversion pulses. Given any standard NMR/MRI sequence, it permits one to modify it in a way which will attenuate, in a predictable manner and before data acquisition, signals arising from components with different r rates ($r = 1/T_1$). Consequently, it is possible to define relatively simple protocols to suppress and/or to quantify signals of different components. This article describes a simple way to construct *low-pass*, *high-pass* and *band-pass* PERFIDI filters. Experimental data are presented in which the method has been used to separate fat and water proton signals. We also present a novel protocol for very fast determination of the ratio between the fat signal and the total signal which avoids any time-consuming magnetization recovery multi-array data acquisition. The method has been validated also for MRI, producing well T_1-contrasted images.

1. Introduction

Many natural and artificial systems, including human tissues, food products and fluid saturated porous media, when analyzed by Nuclear Magnetic Resonance or Magnetic Resonance Imaging (NMR/MRI) methods, present populations of ^{1}H nuclei which all contribute to the acquired signals but exhibit different longitudinal relaxation times (T_1). Methods which allow one to separate such spin populations according to their T_1 are of great practical importance. Typical cases include water and fat in biological tissues, or water and oil in porous media. In MRI one desires to suppress the signals due to fat in order to improve MRI contrast in more relevant tissues. The food industry is interested in the evaluation of the fat-to-lean ratio in meat, and in the petroleum industry one wishes to separate the signals from water and oil present in the pore space of rocks.

In the case of fat–water signal separation, the methods proposed so far [1–13] are based on differences in relaxation times, chemical shift, diffusion coefficients, or on combinations thereof. A very common approach to suppressing particular components is to exploit the differences in T_1. Usually, an inversion recovery sequence with a short inversion time (STIR) [5,6] is used, with the inversion time chosen so as to null the fat magnetization. An extension of STIR is the application of Double Inversion Recovery (DIR) or Multiple Inversion Recovery (MIR) [7–12] to zero the signals associated with more than one T_1 value. The use of these methods based on inversion pulses is particularly useful at low magnetic field intensity, where chemical shift methods are ineffective.

The method applied in this paper also exploits multiple inversion recovery pulses, but it differs substantially from MIR, because it can be considered as a category of r (inverse of T_1) filters based on a different line of reasoning. Its effect is not to zero the signals for a discrete number of T_1 values, but to strongly attenuate the signal in selected ranges of T_1 values, while the remaining signal is affected by a computable attenuation. In other words, the method is an analogue of the electronic *band-pass*, *high-pass* and *low-pass* filters, focusing primarily on the components which *pass through*, rather than on those which are *blocked*.

This approach has been named Parametrically Enabled Relaxation FIlters with Double and multiple Inversion (PERFIDI) [14,15]. Its operational strategy consists in: (i) acquisition of the signals from

* Corresponding author. Fax: +39 051 2095047.
E-mail address: paola.fantazzini@unibo.it (P. Fantazzini).

1090-7807/$ - see front matter © 2010 Elsevier Inc. All rights reserved.
doi:10.1016/j.jmr.2010.07.010

a set of two or more radio-frequency (rf) pulse sequences with particular preambles and (ii) computing a particular linear combination of the acquired data. Each sequence is made of two parts. The first one is the preamble, made of a series of inversion pulses, whose timing is varied depending on the desired filter behavior, while the second one is a standard sequence to which the filter is applied. Fig. 1 shows a diagram of the PERFIDI method based of two sequences (notice the timing differences in the preambles). Being a family of filters, PERFIDI is particularly useful for complex systems, where a continuous distribution of longitudinal relaxation rates r is expected. The choice to use only inversion rf pulses is motivated by the fact that inversion pulses have the largest effect on longitudinal magnetization, have a high tolerance to instrumental imperfections, produce the smallest amount of offset-related artifacts due to transverse magnetization components, can be made more precise by using composite pulses, and are compatible with optional spoiler gradients. Another important aspect of PERFIDI is that it can be used to separate sample components according to their longitudinal relaxation rate *r prior* to the data acquisition rather than having to do it mathematically *a-posteriori* and face the numerical ill-conditioning of Inverse Laplace Transform (ILT) algorithms.

In this paper we present experimental data which demonstrate the performance of the method by applying two-pulse, two-sequence PERFIDI preambles to distinguish and quantify signals of fat and water protons in muscle tissues.

2. Methods

2.1. Mathematics of T_1 filters PERFIDI

In real conditions, on real instruments, the inversion efficiency of rf pulses is limited. The possibility of using PERFIDI in a reliable way even on large samples stems from the fact that its mathematics accounts for the limited inversion efficiency.

The mathematics of the PERFIDI filters has been described in details in Eqs. (4)–(7) in Ref. [15]. Here, the results will be summarized and extended. Let r be the longitudinal relaxation rate of a spin population and η the inversion efficiency, ranging from 1 (perfect inversion) to -1 (no effect). In practice, NMR instruments exhibit η values in the range 0.75–0.95. By applying the Bloch equation for longitudinal relaxation, the longitudinal magnetization after a set of n consecutive elementary blocks with n delays d_j (see Fig. 1) will be:

$$m_f = F(r; d_1, d_2, \ldots, d_n, m_1) = 1 - \sum_{l=0}^{n-1} \{1 + \eta[1 - \delta_{l,n-1}(1 - m_1)]\} \cdot (-\eta)^l \cdot \exp\left(-r \sum_{j=n-l}^{n} d_j\right). \quad (1)$$

Assuming $m_1 = 1$ (i.e. starting with equilibrium magnetization), $F(r; d_1, d_2, \ldots, d_n)$ turns out to be a polynomial with respect to η. It represents the effect of the filter and can be considered as the attenuation produced on the longitudinal magnetization of the r component. To make the effect of the filter the same for all components with the same value of r, regardless of the value of η, it is necessary to separate the effects of η from those of r. It can be demonstrated (see Eq. (6), Ref. [15]) that it is possible, by means of linear combinations (typically just sums and differences) of sequences with different PERFIDI preambles, to achieve a factorization of the type:

$$F(r; d_1, d_2, \ldots, d_n) = F(r, \{d_l\}) = E(\eta) f(r, \{d_l\}), \quad (2)$$

where $E(\eta)$ is a global efficiency factor independent of r and $f(r,\{d_l\})$ is an η-independent *filter profile*.

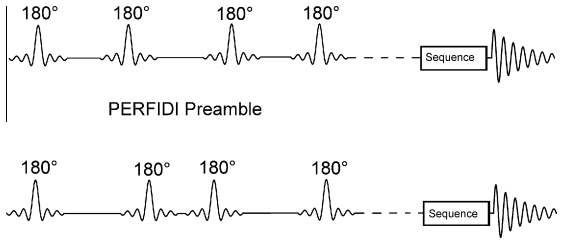

Fig. 1. Schema of a PERFIDI filter based on two rf sequences. The inversion pulses constitute the preamble to the standard sequence. Signals, with the appropriate phase, will be linearly combined to produce the desired filter.

2.2. Two-sequence two-block PERFIDI: conditions to get low-pass, high-pass and band-pass filters

The simplest class of PERFIDI is composed of just two sequences, each made of two elementary PERFIDI blocks. If one acquires two scans using the same delay d_2 in the second block but different delays d_1 and D_1 in the first block and subtracts the two data sets (see Fig. 2), the effect on a component with relaxation rate r is:

$$F(r; d_1, d_2) - F(r, D_1, d_2) = \eta(1 + \eta)(e^{-rd_1} - e^{-rD_1})e^{-rd_2}. \quad (3)$$

In this case one achieves the desired factorization and makes sure that the filter profile will be the same for all sample voxels. For example, if fat is suppressed by the filter in one region of the sample, it will be suppressed everywhere.

Selecting different values of the delays D_1, d_1 and d_2 one can modify the filter profile in various ways. It is obvious that one should set $d_1 < D_1$, otherwise the attenuation would produce either a negative magnetization (when $d_1 > D_1$) or exact zero (when $d_1 = D_1$).

The effect of d_2 is to reduce f, that is to further attenuate the signal, so it is suitable to set $d_2 = 0$, unless further contrast effects between components are needed. The remaining delays determine the kind of filter: $D_1 = \infty$ (in practice $D_1 \approx 5/r$) produces a *low-pass* filter, $d_1 = 0$ a *high-pass* filter, in the other cases a *band-pass* filter is obtained, where the expressions *low-pass*, *high-pass* and *band-pass* refer to the relaxation rate r rather than to the relaxation time T_1. Fig. 3 shows profiles and shifts of the *low-pass* (Fig. 3a) and *high-pass* (Fig. 3b) filters obtained by two-sequences two-inversion pulses with decreasing delays.

The values of D_1 or d_1 required to obtain a filter with a given attenuation f at a given rate r for the *low-pass* and *high-pass* filters are easily computable:

$$d_1 = \frac{1}{r} \ln\left(\frac{1}{f}\right), \text{when } D_1 = \infty, \text{ low-pass filter}, \quad (4)$$

$$D_1 = \frac{1}{r} \ln\left(\frac{1}{1-f}\right), \text{when } d_1 = 0, \text{ high-pass filter}. \quad (5)$$

The *band-pass* filters depend on the choices of both d_1 and D_1, and the analysis is not so straightforward. It is useful to introduce two new parameters k, $k \in [0\text{–}0.5]$, and Δ, in such a way that:

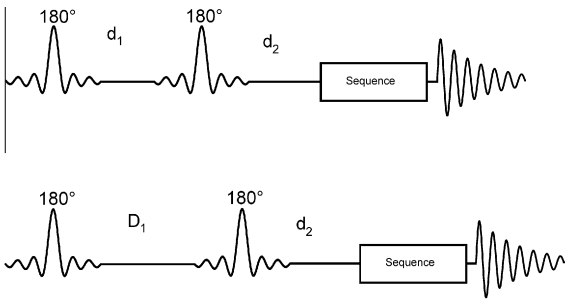

Fig. 2. Schema of two-sequence two-inversion-pulse PERFIDI filter.

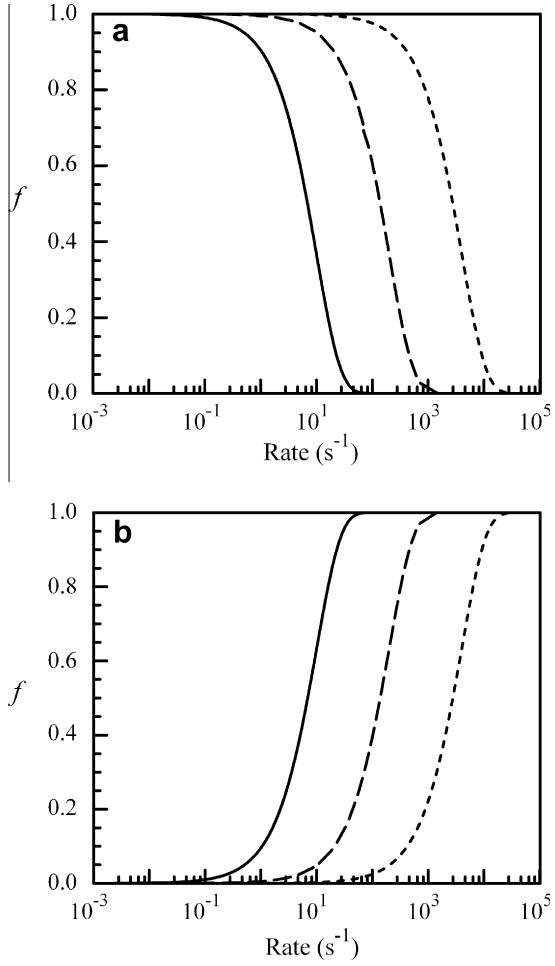

Fig. 3. Profiles and shifts of two-sequence two-inversion-pulse PERFIDI filters (all times in s): (a) *low-pass* filters (longer-relaxation-times-pass) obtained by $D_1 = \infty$ and $d_1 = 0.1$ (solid), 0.005 (dashed), 0.00025 (dotted line); (b) *high-pass* filter (shorter-relaxation-times-pass) obtained by $d_1 = 0$ and $D_1 = 0.1$ (solid), 0.005 (dashed), 0.00025 (dotted line).

$$d_1 = k \cdot \Delta, \quad D_1 = (1-k) \cdot \Delta \quad \text{and} \, f = (e^{-rd_1} - e^{-rD_1}) = (e^{-rk\Delta} - e^{-r(1-k)\Delta}). \tag{6}$$

The parameter k influences the ratio between the two exponents, so it modifies shape and height of the filter. Δ shifts the filter along the horizontal axis, without changing the shape of the filter. Fig. 4 shows the changes of PERFIDI *band-pass* filters as k (a) or Δ (b) are varied. With these new variables, it is easy to demonstrate that the rate r_{peak} for which the filter produces the lowest signal attenuation is

$$r_{peak} = \frac{\ln(\frac{k}{1-k})}{\Delta \cdot (2k-1)} = \frac{\ln(\frac{d_1}{D_1})}{d_1 - D_1}, \tag{7}$$

and the value of the desired attenuation f_{peak} is given by:

$$f_{peak} = \left(\frac{1-k}{k}\right)^{\frac{k}{2k-1}} - \left(\frac{1-k}{k}\right)^{\frac{1-k}{2k-1}}. \tag{8}$$

$$\text{Moreover } \Delta = \frac{\ln\left(\frac{k}{1-k}\right)}{r_{peak} \cdot (2k-1)}. \tag{9}$$

For any relaxation time distributions, the values of the delays d_1 and D_1 to be used to obtain the desired minimum attenuation f_{peak} at the relaxation rate $r = r_{peak}$ can be computed from the previous equations. Using more than two elementary inversion blocks, narrower filters with steeper slopes can be obtained.

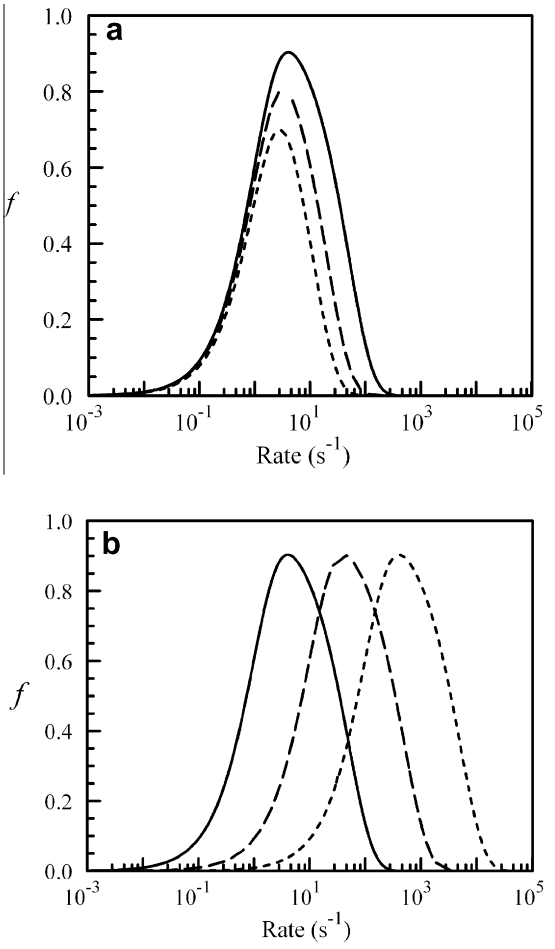

Fig. 4. Signal attenuations due to PERFIDI *band-pass* filters obtained when k (a) and Δ (b) are changed (all times in s). (a) $\Delta = 1$; $k = 0.02$, $d_1 = 0.02$, $D_1 = 0.98$ (solid); $k = 0.05$, $d_1 = 0.05$, $D_1 = 0.95$ (dashed); $k = 0.09$, $d_1 = 0.09$, $D_1 = 0.91$ (dotted line); (b) $k = 0.02$; $\Delta = 1$, $d_1 = 0.02$, $D_1 = 0.98$ (solid), $\Delta = 0.1$, $d_1 = 0.002$, $D_1 = 0.098$ (dashed), $\Delta = 0.01$, $d_1 = 0.0002$, $D_1 = 0.0098$ (dotted line).

3. Experimental

3.1. Quasi-continuos T_1 relaxation time distributions

Longitudinal magnetization relaxation curves were inverted to quasi-continuous relaxation time distributions by 1-Dimensional Inverse Laplace Transform (1D-ILT) computed by the algorithm UPEN [16–18], implemented in the UpenWin software [19]. The UPEN algorithm, differently from others, varies the smoothing factor with relaxation time, in order to maintain the smoothing penalty roughly constant, thus reducing those features of the distributions which are not warranted by the data. Details in the distributions can be suppressed or, in some cases, forced to appear by setting specific parameters of the algorithm to values different from defaults.

3.2. Evaluation of the performance of PERFIDI filters

We have developed a C++ software (i) to predict the effect of the two-sequence two-inversion-pulse PERFIDI filter on any experimental or simulated relaxation time distribution in terms of the attenuation over the distribution and (ii) to determine the best values of the delays to be used in real experiments in order to achieve the desired filtering of the distribution. The input consists of the values of r_{peak} and f_{peak} in the case of band-pass filter, or the values

of the relaxation rate r and the corresponding attenuation f in the cases of low-pass or high-pass filters (see Eqs. (4) and (5)). The filter profile is obtained as output. If the relaxation time distribution function (obtained by relaxation measurements or simulations) is given as input, the total attenuation TA over a given r range is also computed.

3.3. Samples and relaxation NMR measurements

Single samples of muscle tissue for alimentary use and phantoms mimicking the T_1 distributions of muscle tissue were used. Relaxation measurements were performed by means of two different relaxometers. In order to check the response of macromolecular protons of the muscle, a relaxometer characterized by a short dead time (10 μs) and a small sample space (maximum external diameter of the tubes 10 mm) was used. It is based on a Jeol variable-field electromagnet operating at 20 MHz, equipped with a Spinmaster (Stelar, Mede, PV, Italy) data station. A second relaxometer (dead time 140 μs), based on a permanent magnet with a larger bore, operating at 8 MHz, equipped with a portable console (Stelar, Mede, PV, Italy) was used for larger samples, made up of collections of many tubes 10 mm in diameters, put together inside the sample space. The collections of tubes allowed us to mimic the response of muscle tissues with increasing fat content. Two kinds of simulation were performed. In one case, phantoms were made of collections of tubes containing fat and lean meat for alimentary use. In the other case, aqueous solutions at different concentrations of Ethylene-Diamine-Tetraacetic Acid (EDTA) with added paramagnetic ions were used. In our experimental conditions, it was found that typical "muscle" distributions of relaxation times, characterized by different lipid contents, can be obtained by collections (EDTA phantoms) in different proportions of EDTA solutions with T_1 = 30, 70, 270, 350, 470 ms. These relaxation times were chosen in order to mimic the T_1 distributions for tissues containing fat and lean. Longitudinal relaxation data of these EDTA phantoms gave bimodal T_1 distributions when inverted by 1D-ILT. The discrete components with T_1 = 30 and 70 ms, a factor of two apart, could have been resolved. On the contrary, the discrete components with T_1 = 270, 350, 470 ms are too close to each other to be separable. The choice of the input parameters to UpenWin gave the desired bimodal distribution, with one peak contributed by the components with T_1 = 30 and 70 ms and a second one by the remaining three components.

The EDTA phantoms allowed us not only to repeat measurements without sample degradation, but also to vary in a quantifiable manner the ratio between the different signal components and to predict in a verifiable way the effect of the filters. In particular, they were used in order to determine the best value for the delay d_1 in a low-pass filter to suppress the lipid signal in the muscle, to check the hypothesis of no distortion produced in the distribution by a PERFIDI filter with all delays set to zero (zero-PERFIDI), and to check the Fast-PERFIDI method (to be described below). EDTA phantoms were made up of a collection of 5–9 tubes each filled with up to 2 ml of one of the five different solutions.

Standard inversion-recovery sequences (IR: 180° – τ – 90° – FID acquisition – RD) were used to sample the relaxation curve of the longitudinal component of the magnetization of ^{1}H nuclei. FID is the acronym for Free Induction Decay, RD for recycle delay. All curves were acquired using phase-cycling procedures.

On the Jeol relaxometer IR measurements were performed on small pieces of muscle, using the following parameters: pulse duration of 3.5 μs to obtain a nutation angle of $\pi/2$, RD = 4 s; eight excitations. Sixty four FID curves were acquired for increasing values of τ varying from 5 ms to 4.8 s in geometrical progression. All FIDs, acquired on animal muscles obtained at different IR times τ, showed the presence of at least two ^{1}H spin groups distinguishable through the different FID decay shapes: (1) quasi-Gaussian shape (related to fast decay, solid-like group) and (2) exponential decay (slower decay, liquid-like group). In principle, the different behaviors can be ascribed to different (^{1}H or molecular) mobility. FIDs were fit to the sum of a Gaussian and an exponential in order to separate solid and liquid components, by a strategy already used in the past for wood, bone, collagen, hydrated calcium nitrate and cements [20–23]. An accurate determination of the two extrapolated signal amplitudes at each τ can be obtained, to produce separate files to be used as input in UpenWin software in order to obtain, as output, the quasi-continuous T_1 distributions, for both spin groups.

On the second relaxometer the $\pi/2$ pulse duration was 30 μs and the dead time was 140 μs, while other acquisition parameters depended on the samples. For measurements on the collection of animal tissue samples, IR sequences were obtained by 64 FIDs acquired by means of four excitations for increasing values of τ varying from 1 ms to 4 s in geometrical progression. Each of these FIDs was obtained with 200 points sampled every 1 μs after the dead time. Recycle delay was set to 5 s. For measurements on the collection of EDTA aqueous solutions, single FIDs were acquired by means of 64 excitations and a RD of 2.4 s. Each FID was sampled every 2 μs. IR sequences were obtained by 128 (or 64) FIDs acquired by means of 4 (or 8) excitations for increasing values of τ varying from 1 ms to 2.4 s in geometrical progression. Each of these FIDs was sampled every 2 μs. Recycle delay was set to 2.4 s also for IR measurements.

3.4. Low-pass PERFIDI filters for relaxation measurements

A two-sequence two-inversion-pulse low-pass PERFIDI filter was applied as preamble for both FID and IR acquisitions. Delays were chosen as described in the following sections. It will be shown that, in order to quantify the fraction of the total signal in a component by the PERFIDI method, it is necessary to compare the total signals obtained from the same sequence with and without the application of a PERFIDI filter. In order to make this comparison, a more consistent result can be obtained by comparing the signal obtained with a low-pass filter, and the signal obtained with the same filter type, but with d_1 and d_2 set to zero (assuming that the latter sequence produces the same attenuation over the whole T_1 distribution). This assumption would be satisfied in an ideal instrument (one with no B_1 inhomogeneity). In order to check this assumption a test experiment was performed on EDTA phantoms. In all cases but one, the phantoms were prepared to mimic bimodal distributions. The attenuation of the total signal varied in the range 5.1–7.7%, but no distortion was introduced over the entire T_1 range by the preamble when the delays were set to zero. In other words, zero-PERFIDI does not introduce any distortion.

3.5. Samples and Low-pass PERFIDI filters for imaging

Images MRI were acquired by Artoscan (ESAOTE S.p.A., Genova, Italy) equipped with a permanent magnet operating at 8 MHz. The coil "knee-standard" provided as default with Artoscan (internal diameter 12 cm) was used. The phantom was realized with the same tubes used for Relaxometry experiments: 5 tubes with different T_1 arranged side by side (in the order 30, 70, 270, 350, 470 ms). Three transversal sections were acquired, producing in each section a sequence of five circles in gray scale. Special attention was paid to avoid signal saturation in order to obtain comparable data and to maintain linearity in the acquired signals. Two different types of sequences have been employed: standard Spin Echo (SE: 90° – τ – 180°– Echo Acquisition – RD) and Spin Echo modified with inclusion of a PERFIDI preamble. For SE sequence the following parameters have been set: Echo Time = 18 ms; RD = 2000 ms; slice

thickness = 3 mm. For PERFIDI SE additional parameters are needed: D_1 = RD, d_2 = 5 ms hold steady in all acquisitions, three values of d_1 were used (d_1 = 300, 450, 600 ms) in order to vary the position of the low-pass filter.

Two-sequence, two-block PERFIDI method requires to subtract signals of an acquisition (d_1, d_2) from a second acquisition (D_1, d_2): a dedicated software called Arts (which allows also the evaluation of the average of signal intensity over the voxels of a Region Of Interest (ROI)) was used for this purpose.

In order to quantify the effects of the filters, a comparison has been made between the computed ($C\_att = e^{-r(d_1+d_2)}$) and the experimental attenuation (M_att). This last value was determined as the ratio between the signal from a ROI obtained by the PERFIDI sequence and the corresponding obtained by a zero-PERFIDI adapted to imaging.

4. Results

4.1. Relaxation time distributions in real muscle samples

Solid–liquid separation was applied to muscle samples containing fat and lean. Fig. 5 shows a typical example of the T_1 distributions obtained after solid–liquid separation.

In all samples examined it is seen that the solid has one peak with, in some cases, a very low tail or peak at short times, as shown in Fig. 5, while the liquid has two peaks. The solid component can be assigned to macromolecular protons. The peak of the liquid at long relaxation time is at the same time as that of the solid. This is an effect of cross-relaxation between macromolecular protons and muscle water and confirms the hypothesis that the peak of the liquid at longer times is due to water and that the one at shorter times, in the range 30–300 ms, is due to fat ^{1}H nuclei. As a matter of fact, values of fat T_1 are reported of the order of 10^2 ms, varying with the Larmor frequency. T_1 = 200 ms (Ref. [5]) and T_1 = 250 ms (Ref. [7]) are reported at 1.5 T. Recently [24], measurements at 3 T gave T_1 = 282 ms for pure lard, 312 ms for white adipose tissue, 341 ms or 460 ms for the fat component in brown adipose tissue with 83% or 53% fat fraction, respectively.

In order to check qualitatively the assumption that the peak in the range 30–300 ms is due to fat protons, samples made of a mixture of bacon and lean in different proportions as described previously, were prepared. Fig. 6 shows bimodal T_1 distributions obtained at 8 MHz (0.2 T) characterized by a shift to shorter times of both T_1 peaks than those from the 20 MHz (0.47 T) measurements. The area below the peak at shorter times increased as the fraction of fatty meat increased in the sample.

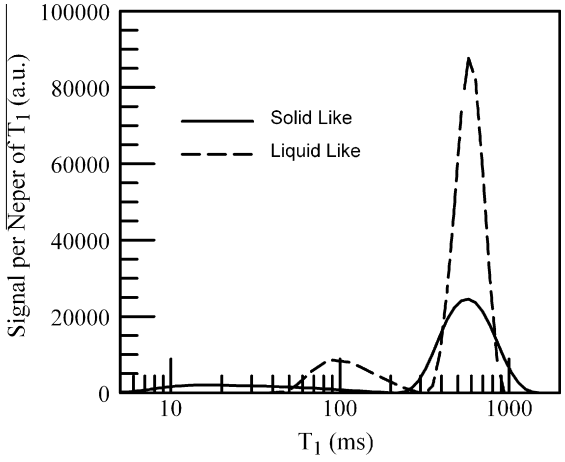

Fig. 5. Quasi-continuous T_1 distributions of the liquid-like (dashed line) and the solid-like (solid line) of a muscle sample. The experimental multi-exponential data are inverted to distributions of relaxation times by the algorithm UPEN. Areas below the distributions are proportional to the numbers of ^{1}H nuclei contributing to the signal. The ordinate is an approximation to (dM)/(d ln T_1), where M is the extrapolated signal per Neper (factor of e) of relaxation time. Measurements at 20 MHz.

4.2. Choice of the PERFIDI filter for EDTA phantoms used to simulate IR signals of muscles with different lipid contents

If the hypothesis that the peak at shorter times in Figs. 5 and 6 is due to fat is correct, a method to suppress the fat signal of a tissue, or to evaluate the signal ratio of fat to water in the tissue could be a two-sequence two-pulse PERFIDI preamble, as represented in Fig. 2, with d_2 = 0, D_1 = RD, and with d_1 to be determined experimentally or by simulation, in order to obtain a low-pass filter, as described by Eq. (6). The choice of the best d_1 was made by using EDTA phantoms prepared by a collection of a discrete number of tubes filled with water solutions at different EDTA concentrations.

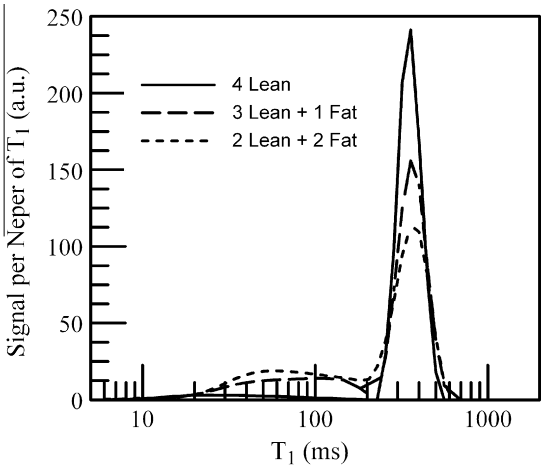

Fig. 6. Quasi-continuous T_1 distributions of the liquid-like component of phantoms prepared with different proportions of fat and lean, in order to mimic tissues with different amount of fat. The experimental multi-exponential data are inverted to relaxation times distributions by means of the algorithm UPEN. Areas below the distributions are proportional to the numbers of ^{1}H nuclei contributing to the signal. These measurements have been obtained at 8 MHz. The amplitudes of the peak at shorter times increase with the amount of fat in the samples, with this peak for the lean sample barely distinguishable from baseline.

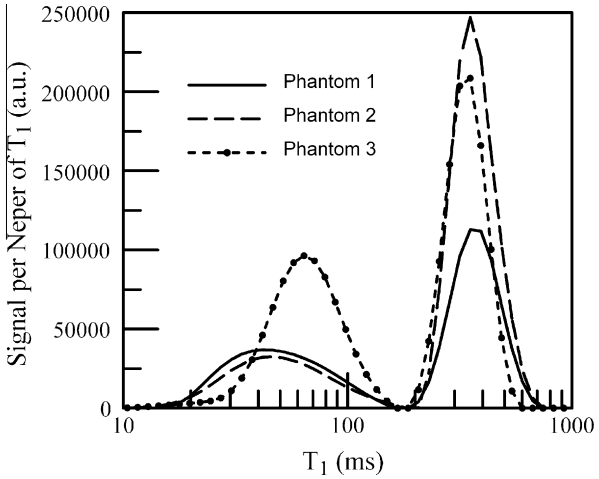

Fig. 7. T_1 distributions of three EDTA phantoms to mimic distributions of fatty tissues with different amount of fat.

Table 1
Comparison between the signal fractions of the two peaks expected by preparation and obtained after inversion of experimental data by UPEN, with the corresponding geometric mean relaxation times, obtained for three EDTA phantoms simulating three muscle tissues with different fat.

EDTA phantom	Fraction expected by preparation		Results from UPEN computations			
	First peak	Second peak	T_{1gm} of the first peak	Fraction of the first peak	T_{1gm} of the second peak	Fraction of the second peak
1	0.40	0.60	48	0.41	371	0.59
2	0.25	0.75	48	0.24	362	0.76
3	0.44	0.56	63	0.44	335	0.56

Fig. 7 shows the T_1 distributions obtained experimentally for three EDTA phantoms. Even though the signals were generated by five discrete components, as expected, bimodal distributions were produced by the algorithm looking for the smoothed distributions from the data inversion.

Table 1 shows, for three EDTA phantoms, the fraction of the two peaks expected by preparation and experimentally computed by UPEN, with the corresponding geometric mean relaxation time ($T_{1gm} = \exp < \ln T_1 >$). The agreement between expected and experimentally computed signal fractions is very good, and the positions of the two peaks at shorter and longer times are consistent with the expected values of fat and water ^{1}H of tissues containing fat.

The PERFIDI software was used to find the best PERFIDI filter to suppress the peak that mimics the fat: low-pass filters with $d_1 = 150$ ms or $d_1 = 300$ ms suppress, at least partially, this peak. As Fig. 8 shows, the peak at longer times is attenuated. The attenuation factor TA depends only on d_1 and on the range of the T_1 values of the lower rate peak. By assuming the range 200–700 ms, the attenuation factors corresponding to $d_1 = 150$ ms and $d_1 = 300$ ms were TA = 0.66 and TA = 0.44, respectively. Fig. 8 shows the results of the simulation on three EDTA phantoms of Fig. 7 with $d_1 = 150$ ms and 300 ms (in both cases $D_1 \cong \infty$).

4.3. FAST-PERFIDI method checked on phantoms used to simulate samples of muscles with different fat contents

If the hypothesis that the short T_1 peak in Figs. 5 and 6 is due to fat signal, a fast determination of fat and water signals is obtained without any time-consuming IR acquisition, by a method we will call FAST-PERFIDI, consisting simply in comparing the two FIDs, one obtained by a normal FID acquisition and another one produced with a low-pass PERFIDI filter. This procedure was tested on the nine EDTA phantoms described in Table 2, whose compositions were determined in such a way as to have a regular increase of the ratio between the first and the second T_1 peak, simulating "fat/(fat + water)" signals. The ratios F/(F + W) obtained by preparation of the EDTA phantoms were in the range 7.7–67%.

The FAST-PERFIDI method consists of the following steps: 1 – acquisition of the FID with a zero-PERFIDI, the extrapolation of the FID to $t_{FID} = 0$ gives S_{ZP}; 2 – acquisition of the FID with a two-pulse two-sequence PERFIDI filter to get a PERFIDI low-pass filter and extrapolation of the FID to $t_{FID} = 0$ to obtain S_P; 3 – computation of the signal assigned to the "water" $S_W = S_P/TA$, where TA, defined previously, is the total attenuation of the "water" peak (TA = 0.66 for $d_1 = 150$ ms and TA = 0.44 for $d_1 = 300$ ms); 4 – computation of the signal from fat: $S_F = S_{zp} - S_w$; 5 – computation of the ratio $F/(F + W) = (S_{ZP} - S_W)/(S_{ZP})$, to be compared with F/(F + W).

Table 2 summarizes the results and compares the predicted and experimental values of the ratios. The tabulated data provide also estimates of the sensitivity and errors associated with this method. Best results have been obtained, as expected, by using the $d_1 = 300$ ms filter, even though it produces an attenuation of the longer T_1 peak by a factor of the order of 44%. In the columns 2 and 3 the total amounts in milliliters are reported of the EDTA solutions having $T_1 = 30$ ms and 70 ms, contributing to the short

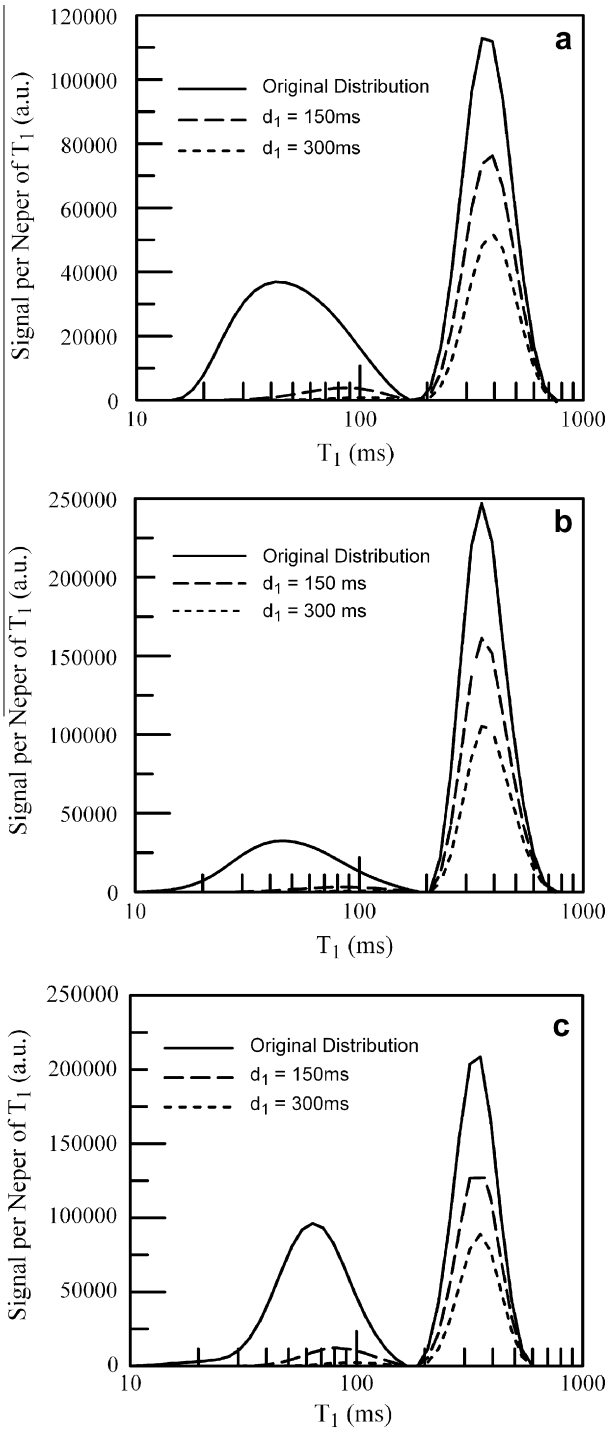

Fig. 8. Application of the preamble PERFIDI shown in Fig. 2, with $d_1 = 150$ ms or 300 ms on IR data acquired on three EDTA phantoms, simulating three muscles with different fat content (in the order from a to c, EDTA phantom #1, #2, #3).

Table 2
Comparison between the "fat fraction", obtained on EDTA phantoms prepared in order to mimic T_1 distributions of muscle samples with different fat content, predicted by preparation F/(F + W) and as obtained by the FAST-PERFIDI method ($F/(F+W)$). The two values separated by semicolons in column five correspond to the two different values of the delay d_1 in the PERFIDI low-pass sequence.

Phantom	Milliliters of EDTA solution contributing to the short T_1 peak (F)	Milliliters of EDTA solution contributing to the long T_1 peak (W)	F/(F + W) (%)	$F/(F+W)$ (%) d_1 = 150 ms; d_1 = 300 ms
C1	12	6	67	56; 62
C2	8.0	12	40	32; 35
C3	6.0	14	30	23; 27
C4	6.0	16	27	20; 23
C5	4.0	18	18	14; 16
C6	3.2	18	15	13; 15
C7	3.2	23	12	10; 12
C8	2.0	18	10	7; 10
C9	1.5	18	7.7	3; 5

T_1 peak, and T_1 = 270, 350 and 470 ms, contributing to the long T_1 peak in the bimodal distributions obtained by the 1D-ILT method.

The agreement between values predicted by preparation and computed by the FAST-PERFIDI method is good for values of the "fat/(fat + water)" signals $\geqslant$10%. The error becomes large for smaller values of the ratio, meaning that, in that case, the assumption of a constant value of the total attenuation TA is no longer valid. In the case of very low fat content one needs a better definition of the distribution of T_1 values in the long T_1 region.

4.4. Validation of PERFIDI in MRI

The applicability to imaging of the two-sequence, two-block PERFIDI has been tested on the same tubes used for Relaxometry. Five tubes put side by side with increasing T_1 (30, 70, 270, 350, 470) from left to right and the choice of transversal section lead up to an image made of a set of circles as shown in Fig. 9. Using SE sequence one expects to obtain the same signal from each sample, due to the linear proportion between signals and proton density. The lowest available Echo Time (18 ms) introduces a light weighting in T_2 that corresponds to a little decrease in the detected signals for T_1 = 30, 70 ms (about 10% and 5%, respectively). Next step is the acquisition of couples of SE sequences with PERFIDI preambles and the following subtractions in order to obtain *low-pass* filters. The images show the suppression of signals from the tubes from the left to the right (from the shorter to the longer T_1) as the delay d_1 is increased from 300 to 600 ms.

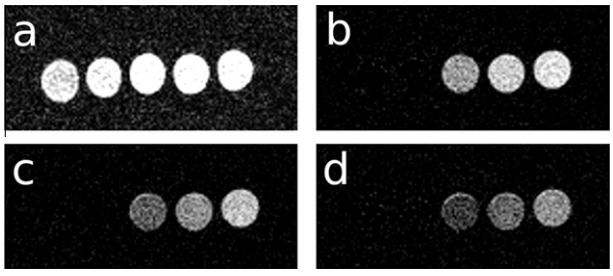

Fig. 9. MRI validation of two-sequence, two-block PERFIDI filter for a phantom simulating T_1 values present in a muscle. (a) SE image of the five test tubes with different T_1 (30, 70, 270, 350, 470 ms from left to right), TE = 18 ms, RD = 2000 ms, slice thickness 3 mm; (b–d) PERFIDI low-pass filtered images with the same set of parameters of SE and D_1 = RD, d_2 = 5 ms, d_1 = 300, 450, 600 ms, respectively. The filter with d_1 = 300 ms (b) zeros the signal that would correspond to fat, with the minimum attenuation introduced on the signal that would correspond to water.

Table 3
Comparison between calculated attenuation ($C\_att = e^{-r(d_1+d_2)}$) – equivalent to the ratio between the residual signals and the original – and measured attenuation (M_att = zero-PERFIDI signal/PERFIDI signal) for each tube and each filter. The top row reports the longitudinal relaxation times of each sample tube. The value 0.00 indicates that the signals in the ROI of the corresponding tube is below the noise level.

	T_1 (ms)	30	70	270	350	470
d_1 = 300 ms	C_att	0.00	0.01	0.33	0.42	0.53
(Fig. 9b)	M_att	0.02	0.03	0.37	0.43	0.49
d_1 = 450 ms	C_att	0.00	0.00	0.19	0.28	0.38
(Fig. 9c)	M_att	0.01	0.02	0.23	0.31	0.40
d_1 = 600 ms	C_att	0.00	0.00	0.11	0.18	0.28
(Fig. 9d)	M_att	0.00	0.01	0.15	0.22	0.32

Even a simple qualitative inspection of the images provides a good idea of the efficiency of the PERFIDI filter in suppressing the shorter T_1 signals, and also allows one to notice the gradual attenuation of the remaining samples. The corresponding quantitative analysis is reported in Table 3, where residual signals after filtering (M_att) are compared with the computed values (C_att). The data analysis shows a substantial agreement between experimental results and theoretical expectations.

5. Conclusions

A common practice to suppress specific sample components is to use inversion-recovery sequences with a Short Inversion Recovery Time, an extension being the Double Inversion Recovery or Multiple Inversion Recovery methods, for zeroing signals of more than one T_1 value. The PERFIDI filters also exploit multiple inversion recovery pulses, but their effect is not to zero the signals of a discrete number of T_1 values, but to suppress the signal over selected ranges of T_1 values, while the remaining signal is affected only by a computable attenuation. Moreover the method produces filters whose profiles are independent of the inversion efficiency of the NMR instrument. Our results show that the method performs well also in large samples.

In this paper we have shown how to produce *high-pass*, *low-pass* and *band-pass* filters, and illustrated the effects of the choices of the delays between inversion pulses. We have also made explicit the dependence of the shape and position of the two-pulse two-sequence PERFIDI filters on the choice of the delays between inversion pulses.

Practical examples have been given of the capability of PERFIDI filters to suppress specific components in multi-component systems characterized by bimodal distributions of longitudinal relaxation times in relaxometry as well as in imaging.

A new method for a fast determination of the ratio of the fat signal to the total signal in muscle tissues has been proposed, based on a comparison of the signal obtained with a low-pass PERFIDI filter and a simple FID. The method avoids the need to use time-consuming magnetization recovery sequences such as IR and a determination of the T_1 relaxation time distribution of the sample. On phantoms prepared to mimic muscle with increasing fat content, the method makes it possible to quantify the ratios "fat/(fat + water)" with relative errors smaller than 15% for all values in the range 10–70%.

The proposed method is applicable also to MR imaging. Here the factorization of the inversion efficiency factor η is also essential. The effect of the filter is the same for all components with the same value of r, regardless of the value of η, which makes it independent on the location of the voxel in the sample.

Acknowledgment

The authors wish to thank R.J.S. Brown for useful discussions.

References

[1] W.T. Dixon, Simple proton spectroscopic imaging, Radiology 153 (1984) 189–194.
[2] J. Ma, F.W. Wehrli, H.K. Song, S.N. Hwang, A single-scan imaging technique for measurement of the relative concentration of fat and water protons and their transverse relaxation times, J. Magn. Reson. 125 (1997) 92–101.
[3] H. Todt, G. Guthausen, W. Burk, D. Schmalbein, A. Kamlowski, Water/moisture and fat analysis by time-domain NMR, Food Chem. 96 (2006) 436–440.
[4] Yi-Qiao Song, A 2D NMR method to characterize granular structure of dairy products, Prog. Nucl. Magn. Reson. Spectrosc. 55 (2009) 324–334.
[5] E. De Kerviler, A. Leroy-Willing, O. Clément, J. Frija, Fat suppression techniques in MRI: an update, Biomed. Pharmacother. 52 (1998) 69–75.
[6] P.M. Jakob, T. Wang, G. Schultz, H. Hebestreit, A. Hebestreit, M. Elfeber, D. Hahn, A. Haase, Magnetization transfer short inversion time inversion recovery enhanced ^{1}H MRI of the human lung, MAGMA 15 (2002) 10–17.
[7] M.D. Does, Relaxation-selective magnetization preparation based on T_1 and T_2, J. Magn. Reson. 172 (2005) 306–311.
[8] W.T. Dixon, M. Sardashti, M. Castillo, G.P. Stomp, Multiple inversion recovery reduces static tissue signal in angiograms, Magn. Reson. Med. 18 (1991) 257–268.
[9] T.W. Redpath, F.W. Smith, Use of a double inversion-recovery pulse sequence to image selectively grey or white brain matter, Br. J. Radiol. 67 (804) (1994) 1258–1263.
[10] M. Mai, J. Knight-Scott, S.S. Berr, Improved visualization of the human lung in ^{1}H MRI using multiple inversion recovery for simultaneous suppression of signal contributions from fat and muscle, Magn. Reson. Med. 41 (1999) 866–870.
[11] M. Mai, Q. Chen, A.A. Bankier, R.R. Edelman, Multiple inversion recovery MR subtraction imaging of human ventilation from inhalation of room air and pure Oxygen, Magn. Reson. Med. 43 (2000) 913–916.
[12] P.A. Boulby, M.R. Symms, G.J. Barker, Optimized interleaved whole-brain 3D Duoble Inversion Recovery (DIR) sequence for imaging the neocortex, Magn. Reson. Med. 51 (2004) 1181–1186.
[13] M.D. Does, J.C. Gore, Compartmental study of T_1 and T_2 in rat brain and trigeminal nerve in vivo, Magn. Reson. Med. 47 (2002) 274–283.
[14] P. Fantazzini, S. Sykora, Italian Patent BO2005A000445 Registered July 1, 2005 by University of Bologna.
[15] S. Sykora, V. Bortolotti, P. Fantazzini, PERFIDI: parametrically enabled relaxation filters with double and multiple inversion, Magn. Reson. Imaging 25 (2007) 529–532.
[16] G.C. Borgia, R.J.S. Brown, P. Fantazzini, Uniform-penalty inversion of multi-exponential decay data, J. Magn. Reson. 132 (1998) 65–77.
[17] G.C. Borgia, R.J.S. Brown, P. Fantazzini, Uniform-penalty inversion of multiexponential decay data II: data spacing, T_2 data, systematic data errors, and diagnostics, J. Magn. Reson. 147 (2000) 273–285.
[18] P. Fantazzini, R.J.S. Brown, Units in distributions of relaxation times, Concepts Magn. Reson. 27A (2) (2005) 122–123.
[19] UpenWin, a Software to Invert Multiexponential Decay Data (villiam.bortolotti@unibo.it).
[20] P. Fantazzini, Magnetic resonance for fluids in porous media at the University of Bologna, Magn. Reson. Imaging 23 (2005) 125–131.
[21] P. Fantazzini, A. Maccotta, M. Gombia, C. Garavaglia, R.J.S. Brown, M. Brai, Solid–liquid NMR relaxation and signal amplitude relationships with ranking of seasoned softwoods and hardwoods, J. Appl. Phys. 100 (2006) 0749071-7.
[22] P. Fantazzini, V. Bortolotti, R.J.S. Brown, M. Camaiti, C. Garavaglia, R. Viola, G. Giavaresi, Two ^{1}H-NMR methods to measure internal porosity of bone trabeculae: by solid–liquid signal separation and by longitudinal relaxation, J. Appl. Phys. 95 (2004) 339–343.
[23] M. Gombia, V. Bortolotti, R.J.S. Brown, M. Camaiti, L. Cavallero, P. Fantazzini, Water vapor absorption in porous media polluted by calcium nitrate studied by time domain nuclear magnetic resonance, J. Phys. Chem. B 113 (2009) 10580–10586.
[24] H.H. Hu, K.S. Nayak, Change in the proton T1 of fat and water in mixture, Magn. Reson. Med. 63 (2010) 494–501.